Structural and Dynamic Information on Double-Decker Yb^{3+} and Dy^{3+} Porphyrin Complexes in Solution through ^1H NMR

Ivano Bertini,*,† Athanassios Coutsolelos,‡ Alexander Dikiy,† Claudio Luchinat,§ Georgios A. Spyroulias,‡ and Anastassios Troganis||

Department of Chemistry, University of Florence, via G. Capponi 7, 50121 Florence, Italy, Chemistry Department, Laboratory of Bioinorganic Chemistry, University of Crete, PO Box 1470, 714 09 Heraklion, Crete, Greece, Institute of Agricultural Chemistry, University of Bologna, Viale Berti Pichat 10, 40127, Bologna, Italy, and NMR Center, University of Ioannina, 451 10 Ioannina, Greece

Received March 28, 1996[⊗]

The ^1H NMR spectra of $[YbH(tpp)_2]$ (**I**), $[DyH(tpp)_2]$ (**II**), [YbH(oep)(tpp)] (**III**), and [DyH(oep)(tpp)] (**IV**), where tpp is tetraphenylporphyrin and oep is octaethylporphyrin, have been analyzed. The aim of this research is to set the limits of information which can be obtained through sophisticated NMR experiments regarding the structure and dynamics in small lanthanide complexes. The phenyl rings have been found to rotate at a rate of about 30 s^{-1} as measured for the $[YbH(tpp)_2]$ complex. The average position of the methyl groups of oep with respect to the porphyrin plane has been determined. Finally, for the dysprosium complexes a structural model in solution has been proposed which fits the pseudocontact shift requirements. Besides mobility, the structure in solution is similar to that in the solid state of the analogous samarium asymmetric complex.

Introduction

Double- and triple-decker lanthanide(III) porphyrin complexes have often attracted the interest of NMR spectroscopists.[1−5] Recently, the characterization of a series of double-decker lanthanide(III) oep and tpp porphyrin complexes, where tpp is tetraphenyl porphyrin and oep is octaethyl porphyrin has been reported.[6] A schematic structure of the complexes is shown in Figure 1. The complexes are neutral due to the presence of a proton on one of the porphyrin nitrogens (not shown).[6] The X-ray structure of the [SmH(oep)(tpp)] complex is available.[7] We intend here to use the ^1H NMR approach to obtain structural and dynamic information in solution on the following complexes: $[YbH(tpp)_2]$ (**I**), $[DyH(tpp)_2]$ (**II**), [YbH(oep)(tpp)] (**III**), and [DyH(oep)(tpp)] (**IV**). Yb^{3+} and Dy^{3+} are known to provide sharp ^1H NMR line widths despite their paramagnetic nature.[8−10] We have used the 1D NOE technique as well as NOESY, ROESY, TOCSY, and COSY experiments tailored to detect connectivities in paramagnetic systems.[11] The aim of the research is that of trying our best to learn about structural and dynamic properties of these complexes in solution after the recent achievement of obtaining solution structures of paramagnetic metalloproteins.[12] Indeed, the solution structure of small complexes is a hard task owing to the lack of constraints as compared to the structure determination of proteins, which have a compact structure. Finally, by using the pseudocontact shifts experienced by some protons in the dysprosium(III) complexes, we have proposed a structural model in solution.

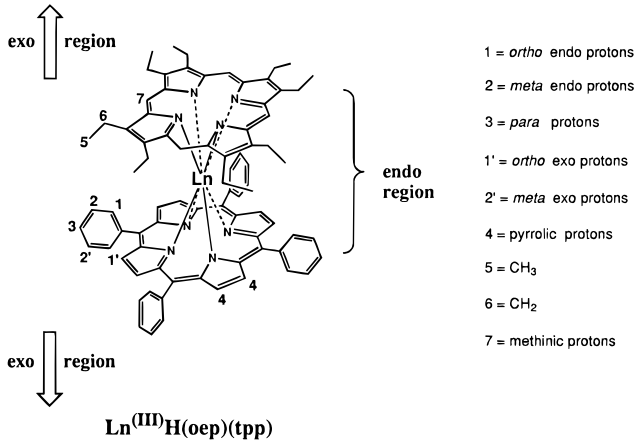

Figure 1. Schematic representation of the asymmetric [LnH(oep)(tpp)] complexes and labeling of proton positions.

Experimental Section

Complexes **I**−**IV** were synthesized according to previously published methods.[6] The samples for NMR spectroscopy were prepared by dissolving **I**−**IV** in deuterated chloroform.

The NMR spectra were recorded using MSL 200, DRX 500, and AMX 600 Bruker spectrometers operating at 200.13, 500.13, and 600.14

† University of Florence.
‡ University of Crete.
§ University of Bologna.
|| University of Ioannina.
⊗ Abstract published in *Advance ACS Abstracts,* September 1, 1996.

(1) Buchler, J. W.; De Cian, A.; Fischer, J.; Kihn-Botulinski, M.; Paulus, H.; Weiss, R. *J. Am. Chem. Soc.* **1986**, *108*, 3652−3659.
(2) Buchler, J. W.; Kihn-Botulinski, M.; Loffler, J.; Wicholas, M. *Inorg. Chem.* **1989**, *28*, 3770−3772.
(3) Buchler, J. W.; De Cian, A.; Fischer, J.; Hammerschmitt, P.; Loffler, J.; Scharbert, B.; Weiss, R. *Chem. Ber.* **1989**, *122*, 2219−2228.
(4) Buchler, J. W.; Loffler, J.; Wicholas, M. *Inorg. Chem.* **1992**, *31*, 524−526.
(5) Buchler, J. W.; Nawra, M. *Inorg. Chem.* **1994**, *33*, 2830−2837.
(6) Spyroulias, G. A.; Coutsolelos, A. G. *Inorg. Chem.* **1996**, *35*, 1382−1385.
(7) Spyroulias, G. A.; Coutsolelos, A. G.; Raptopoulou, C. P.; Terzis, A. *Inorg. Chem.* **1995**, *34*, 2476−2479.
(8) Barry, C. D.; North, A. C. T.; Glasel, J. A.; Williams, R. J. P.; Xavier, A. V. *Nature* **1971**, *232*, 236−245.
(9) Bertini, I.; Luchinat, C. *NMR of paramagnetic molecules in biological systems*; Benjamin/Cummings: Menlo Park, CA, 1986.
(10) La Mar, G. N. In *NMR of Paramagnetic Molecules*; La Mar, G. N., Horrocks, W. D., Jr., Holm, R. H., Eds.; Academic Press: New York, 1973.
(11) Bertini, I.; Luchinat, C. *Coord. Chem. Rev.* **1996**, *150*.
(12) Bertini, I.; Dikiy, A.; Kastrau, D. H. W.; Luchinat, C.; Sompornpisut, P. *Biochemistry* **1995**, *34*, 9851−9858.

S0020-1669(96)00339-4 CCC: $12.00

MHz Larmor frequencies, respectively. The spectra were calibrated by assigning the residual chloroform signal at 298 K a shift from TMS of 7.23 ppm.

Longitudinal relaxation rates were measured using a non selective inversion recovery pulse sequence.[13] The T_1 values were obtained from a two-parameter fit of the data to an exponential recovery function. In every case the magnetization recovery was found to be exponential within the accuracy of the experiment, as expected for fast relaxing nuclei with little cross relaxation and favorable chemical exchange conditions.[14,15]

1D NOE spectra were recorded in difference mode using previously described acquisition schemes.[16,17] Recycle delays and irradiation times ranged from 50 to 350 ms and from 20 to 200 ms, respectively.

2D COSY spectra were recorded in magnitude mode,[18] with recycle delays varying from 100 to 300 ms and t_{1max} and t_{2max} varying from 2 to 5 ms. Under these circumstances cross-peak intensities between signals as broad as 400 Hz were optimized. A nonshifted squared sine bell window function was used to process the data.

2D TOCSY,[19] NOESY,[20] and ROESY[21] experiments optimized for the detection of the connectivities between the hyperfine shifted signals[11,22,23] were recorded in phase sensitive mode. Spectra were acquired with 512 points in the f_1 dimension, from 8 to 128 scans per experiment, and 2K data points in the f_2 dimension. The TOCSY spin lock times ranged from 25 to 40 ms in order to optimize the observation of the scalar connectivities for signals with line widths ranging from 10 to 30 Hz. The NOESY mixing times ranged from 3 to 40 ms. The ROESY spin lock times ranged from 15 to 40 ms. In order to maximize the intensities of the cross-peaks in 2D spectra recorded in the phase-sensitive mode, the data matrices were multiplied by a phase-shifted squared sine bell window function in both dimensions, prior to Fourier transformation.

Heteronuclear $^1H-^{13}C$ HMQC spectra[24,25] were acquired both in magnitude and in phase-sensitive mode using a 5 mm reverse detection probe. The spectra were accumulated with 512 points in the f_1 dimension and 1024 points in the f_2 dimension, by using 128−256 scans per experiment. The refocusing time was 2 ms, and the recycle time ranged from 200 to 400 ms. The WALTZ-16 pulse sequence[26] was used to decouple the carbon nuclei during acquisition. Carbon chemical shifts were calibrated by assigning the residual chloroform signal at 298 K a shift from TMS of 77.7 ppm.

The standard Bruker software package was used for data processing.

The magnetic susceptibility tensors were determined using the program "Fantasia".[27] The chemical shift values of the diamagnetic [LuH(oep)(tpp)] complex[6] were used to calculate the hyperfine shifts for complexes **I**−**IV**.

(13) Vold, R. L.; Waugh, J. S.; Klein, M. P.; Phelps, D. E. *J. Chem. Phys.* **1968**, *48*, 3831−3832.
(14) La Mar, G. N.; de Ropp, J. S In *Biological Magnetic Resonance*; Berliner, L. J., Reuben, J., Eds.; Plenum Press: New York, 1993; Vol. 12, pp 1−78.
(15) Bertini, I.; Donaire, A.; Luchinat, C.; Rosato, A. Submitted for publication.
(16) Banci, L.; Bertini, I.; Luchinat, C.; Piccioli, M.; Scozzafava, A.; Turano, P. *Inorg. Chem.* **1989**, *28*, 4650−4656.
(17) Dugad, L. B.; La Mar, G. N.; Banci, L.; Bertini, I. *Biochemistry* **1990**, *29*, 2263−2271.
(18) Aue, W. P.; Bartholdi, E.; Ernst, R. R. *J. Chem. Phys.* **1976**, *64*, 2229−2235.
(19) Bax, A.; Davis, D. G. *J. Magn. Reson.* **1985**, *65*, 355−360.
(20) Macura, S.; Ernst, R. R. *Mol. Phys.* **1980**, *41*, 95.
(21) Bax, A.; Davis, D. G. *J. Magn. Reson.* **1985**, *63*, 207−213.
(22) Banci, L.; Bertini, I.; Luchinat, C. In *Methods in Enzymology*; James, T. L., Oppenheimer, N. J., Eds.; Academic Press, Inc.: London, 1994; pp 485−514.
(23) Luchinat, C.; Piccioli, M. In *NMR of Paramagnetic Macromolecules. NATO ASI Series*; La Mar, G. N., Ed.; Kluwer Academic: Dordrecht, The Netherlands, 1995; pp 1−28.
(24) Bax, A.; Griffey, R. H.; Hawkins, B. L. *J. Am. Chem. Soc.* **1983**, *105*, 7188−7190.
(25) Bax, A.; Griffey, R. H.; Hawkins, B. L. *J. Magn. Reson.* **1983**, *55*, 301−315.
(26) Shaka, A. J.; Keeler, J.; Frenkiel, T.; Freeman, R. *J. Magn. Reson.* **1983**, *52*, 335−338.
(27) Banci, L.; Bertini, I.; Bren, K. L.; Cremonini, M. A.; Gray, H. B.; Luchinat, C.; Turano, P. *JBIC* **1996**, *1*, 117−126.

Table 1. ^1H NMR Data and Signal Assignment of the [YbH(tpp)$_2$] (**I**) Complex in $CDCl_3$ at 298 K

signal (intens)	obsd chem. shift, ppm	hyperfine shift, ppm	T_1,[a] ms	assignment
A (8)	9.2	1.1	288.6	*meta*
B (8)	8.4	−1.0	31.2	*ortho*
C (8)	8.1	0.9	288.9	*meta*
D (8)	7.1	−0.6	411.8	*para*
E (8)	7.0	0.6	37.8	*ortho*
F (16)	−22.5	−30.6	14.5	pyrrolic

[a] Measured at 500 MHz.

Table 2. ^1H NMR Data and Signal Assignment of the [DyH(tpp)$_2$] (**II**) Complex in $CDCl_3$ at 298 K

signal (intens)	obsd chem. shift, ppm	hyperfine shift, ppm	T_1,[a] ms	assignment
A (8)	21.5	15.1	4.9	exo-*ortho*
B (8)	7.3	0.1	36.3	exo-*meta*
C (8)	−2.0	−9.7	53.6	*para*
D (8)	−10.4	−18.5	28.1	endo-*meta*
E (8)	−50.3	−59.7	3.7	endo-*ortho*
F (16)	−52.9	−61.0	2.8	pyrrolic

[a] Measured at 500 MHz.

Table 3. ^1H NMR Data and Signal Assignment of the [YbH(oep)(tpp)] (**III**) Complex in $CDCl_3$ at 298 K

signal (intens)	obsd chem. shift, ppm	hyperfine shift, ppm	T_1,[a] ms	assignment
A (4)	39.5	30.4	8.0	*meso*
B (8)	29.5	25.4	13.9	endo−CH_2
C (8)	21.1	17.4	18.7	exo−CH_2
D (4)	10.7	1.3	21.7	endo-*ortho*
E (4)	10.1	3.7	34.0	exo-*ortho*
F (4)	8.4	0.8	251.3	*para*
G (4)	6.8	−1.3	150.7	endo-*meta*
H (4)	6.1	−1.1	157.6	exo-*meta*
I (24)	3.7	2.4	40.2	CH_3
J (8)	-19.9	−28.0	9.3	pyrrolic

[a] Measured at 500 MHz.

Table 4. ^1H NMR Data and Signal Assignment of the [DyH(oep)(tpp)] (**IV**) Complex in $CDCl_3$ at 298 K

signal (intens)	obsd chem. shift (283 K), ppm	hyperfine shift, ppm	T_1,[a] ms	assignment
A (4)	22.6	16.2	3.4	exo-*ortho*
B (4)	3.8	−3.4	30.1	exo-*meta*
C (4)	−1.9	−9.6	52.6	*para*
D (24)	−2.5	−3.8	9.3	CH_3
E (8)	−2.5 (-4.0)	−6.6	7.2	CH_2
F (8)	−4.4 (−5.9)	−8.2	7.5	CH_2
G (4)	−12.6	−21.7	1.5	*meso*
H (4)	−13.8	−21.9	31.9	endo-*meta*
I (4)	−49.9	−59.3	4.0	endo-*ortho*
J (8)	−61.4	−69.5	2.4	pyrrolic

[a] Measured at 500 MHz.

Results and Discussion

The NMR assignment was achieved using similar procedures for all complexes, as discussed later. The assignments are reported in Tables 1−4. All signals are observed except for the acidic proton that is expected to be very close to the metal according to what was found in the diamagnetic analog.[6] As the assignment of the symmetric complexes is rather straightforward, we will describe it first, and then we will take advantage of it for the assignment of the asymmetric complexes. The stereospecific assignment of methylene and phenyl protons is discussed later.

Symmetric [YbH(tpp)$_2$] (I) and [DyH(tpp)$_2$] (II) Complexes. The signals of both Yb^{3+} and Dy^{3+} complexes are affected by the presence of the unpaired electrons ($S = {}^1/_2$, $J =$

$^7/_2$, $g_J = {}^8/_7$ for Yb^{3+} and $S = {}^5/_2$, $J = {}^{15}/_2$, and $g_J = {}^4/_3$ for Dy^{3+}) which cause nuclear relaxation rate enhancements and isotropic hyperfine shifts. The larger paramagnetism of the dysprosium(III) complexes results in larger chemical shifts and shorter T_1 with respect to the ytterbium(III) complexes. Comparison of the signal intensities reveals that the upfield shifted signals F in both complexes (Tables 1 and 2) have twice the intensity of all of the other signals. This allows us to unambiguously assign signals F to the pyrrolic protons. The ^{1}H NMR assignment of phenyl protons is achieved by 2D TOCSY, NOESY, and ROESY experiments (data not shown). 2D TOCSY experiments unravel the connectivities among all aromatic protons, while NOESY and ROESY maps display strong exchange cross-peaks between diastereotopic *ortho* and *meta* proton pairs. Chemical exchange is detected in NOE and ROE types of experiments through positive 2D cross-peaks, whereas the effect is negative in 1D experiments. The *meta* and *ortho* proton signals can be easily distinguished by their different longitudinal relaxation times, as the *ortho* protons are closer to the metal and, hence, have shorter relaxation times than the *meta* protons. This assignment is confirmed by small negative NOESY cross-peaks between *para* and *meta* protons and negative ROESY cross-peaks between *para* and *meta* and *meta* and *ortho* protons. As seen from the dependence of the NOE and ROE effects on the correlation times,[28,29] the NOE can be positive or negative (and, by convention, the NOESY cross-peak negative or positive) depending on whether $\omega_I\tau_c$ is smaller or larger than unity, whereas the ROE is always positive (the ROESY cross-peak is always negative). The sign of the dipolar connectivities can therefore provide information on the dynamics of a molecule: positive NOE (negative NOESY) connectivity indicates that the molecule is in the fast motion limit, whereas the reversed sign of the cross-peaks underlines that the molecule is in the slow motion limit. The present system is in the fast motion limit, a τ_c of 3×10^{-10} s being estimated from the intensity of the NOESY and ROESY cross-peaks. It was earlier reported that some iron-containing porphyrinate complexes are in the slow motion limit[30−32] according to the signs of their 1D NOE and 2D NOESY connectivities between pyrrolic protons (which in that case are inequivalent). This point will be further considered later.

The observation of five phenyl ring protons is indicative of slow flipping rate of the phenyl rings compared to the chemical shift differences. On the other hand, the substantial similarity of the T_1 values within each diastereotopic pair (Tables 1 and 2) suggests that the flipping rate is fast on the relaxation time scale. The intensity of NOESY (or ROESY) cross-peaks between the two *ortho* or the two *meta* protons allows us to estimate the flip rate of the ring to be around 30 s^{-1} from the equation[28,29]

$$I_{AB}/I_{AA} = (1 - \exp\{-2k\tau_m\})/(1 + \exp\{-2k\tau_m\}) \quad (1)$$

where I_{AA} and I_{AB} are the intensities of the diagonal and cross-peaks, respectively, τ_m is the mixing time, and k is the exchange rate. The obtained value for the phenyl ring flip rate is in good agreement with that found for the [Ru(CO)(*i*-Pr-tpp)] complex of 60 s^{-1} at 95 °C.[33] As the reciprocal flip rate of the rings determined above is much longer than the τ_c value of about 3×10^{-10}s estimated above for the dipolar interactions within the phenyl ring, the obtained τ_c must reflect the overall rotational correlation time of the molecule.

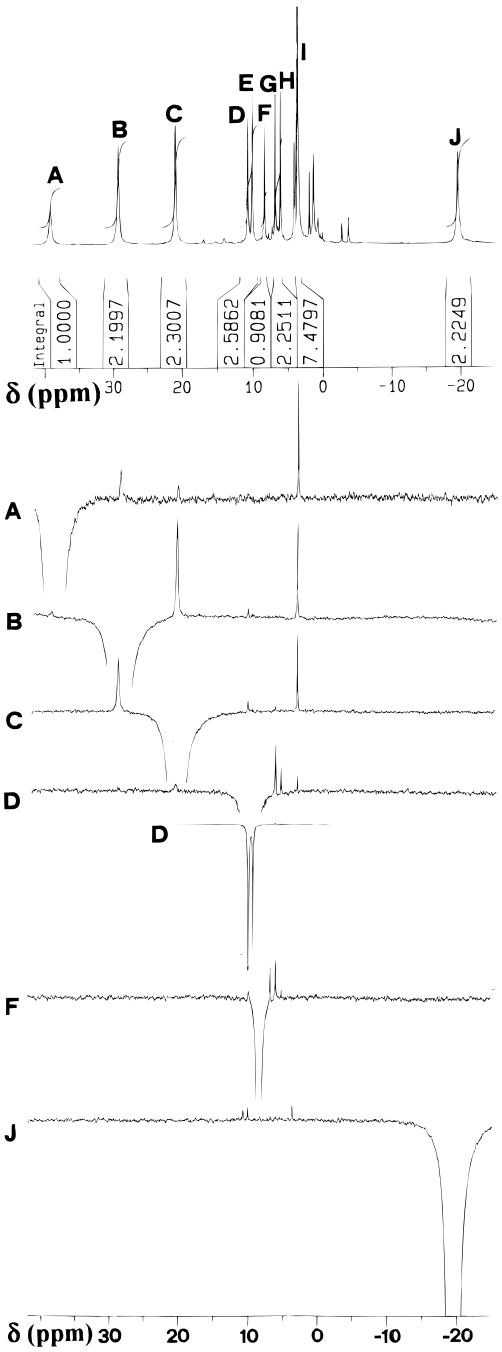

Figure 2. 500 MHz 298 K ^{1}H NMR spectra of [YbH(oep)(tpp)] (**III**) in deuterated chloroform. The upper trace represents the reference spectrum with signal integrals. The other traces are 1D NOE difference spectra. The traces are labeled according to the saturated signals. The 1D NOE difference spectra were obtained with the *on*−*off*(*left*)−*on*−*off*(*right*) acquisition scheme described earlier.[16,17] In this way, negative responses from signals even very close to the irradiated signal (as in the case of the D→E saturation transfer) are reliable because off-resonance effects are opposite in sign.

The [YbH(oep)(tpp)] (III) Complex. The proton chemical shifts and T_1 values of **III** are reported in Table 3, while the NMR spectrum is shown in the upper trace of Figure 2. As

(28) Noggle, J. H.; Schirmer, R. E. *The Nuclear Overhauser Effect*; Academic Press: New York, 1971.
(29) Neuhaus, D.; Williamson, M. *The Nuclear Overhauser Effect in Structural and Conformational Analysis*; VCH: New York, 1989.
(30) Simonis, U.; Lin, Q.; Tan, H.; Barber, R. A.; Walker, F. A. *Magn. Reson. Chem.* **1993**, *31*, S133−S144.
(31) Tan, H.; Simonis, U.; Shokhirev, N. V.; Walker, F. A. *J. Am. Chem. Soc.* **1994**, *116*, 5784−5790.
(32) Basu, P.; Shokhirev, N. V.; Enemark, J. H.; Walker, F. A. *J. Am. Chem. Soc.* **1995**, *117*, 9042−9055.
(33) Eaton, S. S.; Eaton, G. R.; Holm, R. H. *J. Organomet. Chem.* **1972**, *39*, 179−195.

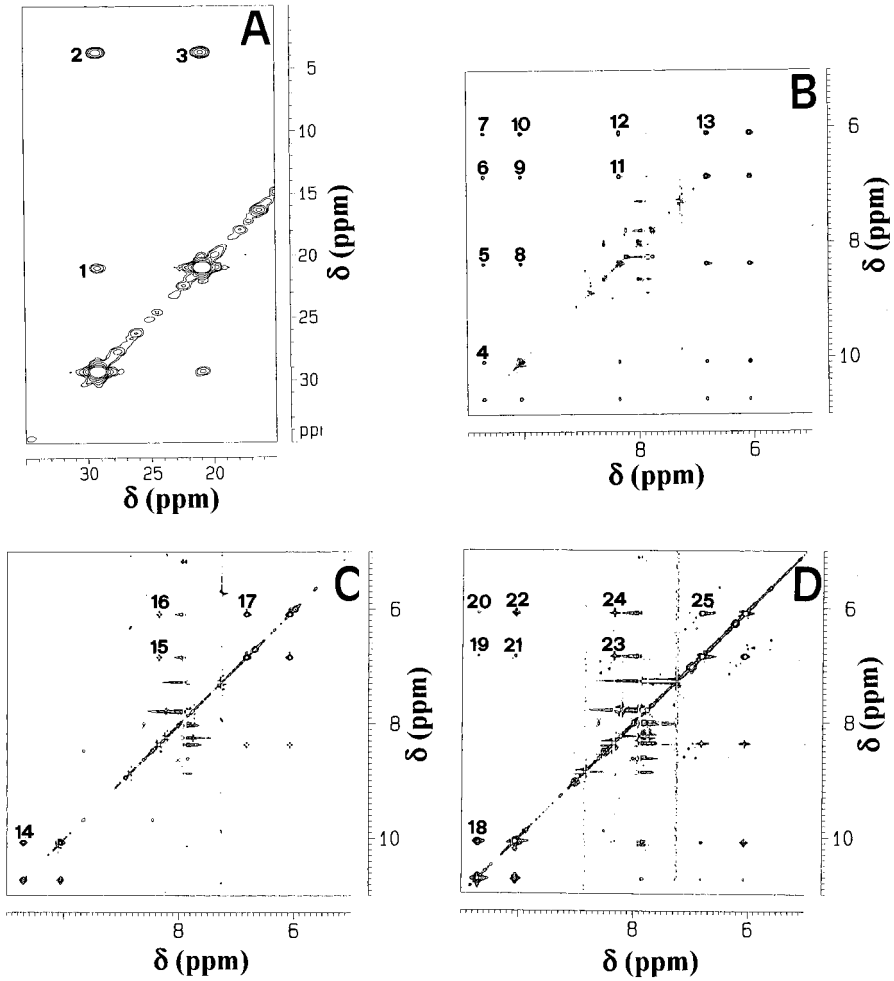

Figure 3. 500 MHz 298 K ^{1}H NMR spectra of [YbH(oep)(tpp)] (**III**). (A) 2D COSY spectrum. Cross-peak assignments: (1) endo $-CH_2$, exo $-CH_2$; (2) endo $-CH_2$, $-CH_3$; (3) exo $-CH_2$, $-CH_3$. (B) 2D TOCSY spectrum with spin lock time of 40 ms. Cross-peak assignments: (4) endo-*ortho*, exo-*ortho*; (5) endo-*ortho*, *para*, (6) endo-*ortho*, endo-*meta*; (7) endo-*ortho*, exo-*meta*; (8) exo-*ortho*, *para*; (9) exo-*ortho*, endo-*meta;* (10) exo-*ortho*, exo-*meta;* (11) *para*, endo-*meta*; (12) *para*, exo-*meta*; (13) endo-*meta*, exo-*meta*. (C) 2D NOESY spectrum with mixing time of 40 ms. Cross-peak assignments: (14) endo-*ortho*, exo-*ortho*; (15) *para*, endo-*meta*; (16) *para*, exo-*meta*; (17) endo-*meta*, exo-*meta*. (D) 2D ROESY spectrum with spin lock time of 20 ms. Cross-peak assignments: (18) endo-*ortho*, exo-*ortho*; (19) endo-*ortho*, endo-*meta*; (20) endo-*ortho*, exo-*meta*; (21) exo-*ortho*, endo-*meta*; (22) exo-*ortho*, exo-*meta*; (23) *para*, endo-*meta*; (24) *para*, exo-*meta*; (25) endo-*meta*, exo-*meta*.

can be seen from the figure the spectrum consists of more signals than expected. Some weak signals are due to impurities, present as minor species (probably due to free porphyrins). They are typical of diamagnetic organic molecules and easily distinguished also on the basis of shifts and relaxation properties. Some hints for the assignment come from the comparison of the T_1 values and by taking advantage of the X-ray structure of the analogous complex with Sm^{3+}.[7] Signals A, B, C. and J, having the shortest relaxation times and being most shifted from the diamagnetic spectral region (0−10 ppm), should correspond to $-CH_2$ and *meso* protons of oep and pyrrolic protons of tpp, while the other signals (D, E, F, G, H, I) are expected to correspond to methyl (oep ring) and phenyl (tpp ring) protons, which are farther from the metal ion. Among the first group of signals, signal A with an intensity of 4 can be assigned to the *meso* protons of oep, while signal J can be assigned to the pyrrole protons of tpp by analogy with the symmetric complex. Signals B and C therefore belong to the methylene pairs of oep. Among the second group of signals, signal I is assigned to the methyl group of oep on the basis of its intensity.

The above assignment is confirmed by 1D NOE and 2D (COSY, TOCSY, NOESY and ROESY) experiments adjusted for the detection of fast relaxing signals.

The 2D homonuclear COSY map is shown in Figure 3A. The scalar connectivities observed in the downfield region of the spectrum (cross-peaks 1, 2, and 3) confirm protons B, C, and I to belong to the geminal methylene protons and methyl protons, respectively. 1D NOE difference spectra at 500 MHz (Figure 2) show that by saturating signals B and C, dipolar connectivities with signals C and I and with B and I, respectively, are observed. Moreover, some small NOEs with aromatic protons (B→D, C→D, C→G) are also observed. If the *meso* signal A is saturated, connectivities with signals B, C, and I are detected. Neither scalar (data not shown) nor dipolar connectivities (excluding small NOEs with signals D, E, and I (Figure 2)) are observed for the pyrrole signal J. The positive NOE's observed in the 1D NOE experiments again indicate that the molecule is in the fast motion limit. The structural information contained in these NOE's will be further discussed later.

A comment is due about the faster rotational correlation times of the present systems as compared to the slightly smaller iron−porphyrin systems under similar experimental conditions.[30−32] The difference is not very large but is particularly meaningful as these two classes of compounds fall at the opposite sides of the positive−negative NOE threshold given by $\omega_I\tau_c = 1$. A tentative explanation might invoke the inadequacy of the Stokes−Einstein approximation ($\tau_R \propto$ MW) in these relatively small molecules. It could be that the solvodynamic properties of the relatively compact double-decker compounds allow their

somewhat faster rotation with respect to the iron−porphyrin complexes with axial ligands stretching out considerably from the center of the molecule.

The 2D TOCSY map (Figure 3B) allowed us to find scalar connectivities between aromatic protons of the tpp ring (cross-peaks 4−13). The assignment of these protons comes from the combination of 2D TOCSY, NOESY (Figure 3C) and ROESY (Figure 3D) experiments. The very strong positive NOESY cross-peaks 14 and 17 indicate that they are due to exchange within the *ortho* and *meta* proton pairs and leave signal F to be assigned as the *para* proton. The different longitudinal relaxation times of the signals D, E, G, and H (Table 3) and the small negative NOESY cross-peaks 15 and 16 with the *para* proton F allow us to assign the latter two protons as due to *meta* and, consequently, the former two as due to *ortho* protons of the aromatic ring. This assignment is further confirmed by the 1D NOEs obtained by saturating some of the aromatic protons. In Figure 2, as an example, the 1D NOE difference spectrum obtained upon saturation of signal D is shown. We observe strong (about 35%) negative effect (saturation transfer) with its diastereotopic partner E, while the NOEs with signals G and H (diastereotopic *meta* pair) are small and positive, as expected for dipolar connectivities in the fast motion limit.

The assignment of aromatic protons obtained from the 2D NOESY spectrum is further confirmed by the 2D ROESY spectrum (Figure 3D). Indeed, additional cross-peaks (cross-peaks 19−22) with respect to the NOESY map are observed. These latter peaks refer to the dipolar connectivities between *ortho* protons and *meta* protons pairs.

The comparison of the chemical shifts and T_1 values for **I** and **III** reveal that the corresponding values in both complexes are rather similar although not identical. The observed small differences between the two complexes can be either due to a slight difference in magnetic anisotropy or to minor structural differences.

The [DyH(oep)(tpp)] (IV) Complex. The proton chemical shifts of **IV** are reported in Table 4, and the 298 K NMR spectrum is shown in the upper trace of Figure 4. Taking advantage of the different intensities of the signals reported in Table 4 and Figure 4 and of the similarity in the chemical shifts with **II**, we can assign signal J as due to pyrrolic protons, signal D as due to methyl protons, and, finally, signals E and F as due to methylene protons.

Again, the T_1 values (Table 4) allow us to distinguish between the signals of the complex and those of impurities, and give us further hints for the assignment. For example, the broad signal G at −12.6 ppm has the shortest relaxation time (1.5 ms). Obviously neither scalar nor dipolar connectivities can be detected for this signal. However, as appears from the X-ray structure[7] the closest protons to the metal ion are the *meso* protons. Therefore, we assign signal G as due to the *meso* protons of oep.

The 1D NOE spectra obtained by saturating signals A, H, and I are shown in Figure 4. Upon saturation of signal A a strong negative connectivity with signal I is observed, and vice versa. An intense negative response in the 1D NOE spectra is also observed between signals H and B. A decrease of temperature results in a decrease of the intensities of these negative peaks (data not shown). This is consistent with the observed negative peaks being due to saturation transfer. Therefore, signals A, B, H, and I should correspond to *ortho* and *meta* protons of the aromatic ring, which are the only ones capable of giving rise to saturation transfer as already noted for the Yb^{3+} complexes. In the 2D COSY spectrum (Figure 5A) we observe cross-peaks between signals A and B and

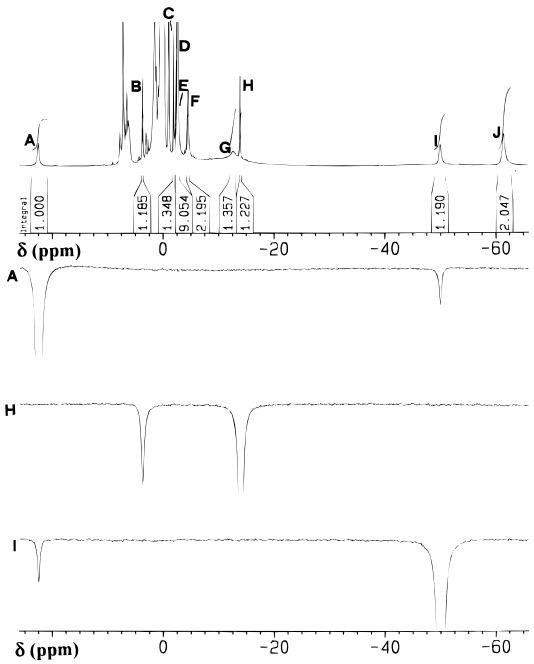

Figure 4. 500 MHz 298 K ^{1}H NMR spectra of [DyH(oep)(tpp)] (**IV**) in deuterated chloroform. The upper trace represents the reference spectrum with signal integrals. The other traces are 1D NOE difference spectra. The traces are labeled according to the saturated signals.

between H and I (cross-peaks 26 and 28). This allows us to assign signals A and I, as well as B and H, as *ortho* and *meta* protons, respectively. We then assign signal C as due to the *para* proton on the basis of its scalar connectivities with one of the *meta* protons at 3.8 ppm in the COSY and TOCSY maps (Figure 5A,B, cross-peaks 27 and 29) (another *meta* proton was out of the spectral window of the TOCSY experiment). This assignment is also consistent with the ^{1}H−^{13}C (natural abundance) HMQC experiment (Figure 5C), where the corresponding carbon signals fall in the aromatic region. We also note that the pattern of the aromatic proton shifts is analogous for **II** and **IV**, and follows the order: *ortho*−*meta*−*para*−*meta*−*ortho*.

We are left, thus, with the two unassigned signals E, overlapped at 298 K with D and partially resolved at lower temperatures, and F. By exclusion, we assign these signals to methylene protons. Their similar T_1 values do not allow us to perform the stereospecific assignment.

Comparing the shift and T_1 values for **II** and **IV** we observe that the corresponding values are quite similar (Tables 2 and 4), even more so that those of **I** and **III**, which would indicate that the distances between the protons and the metal ion in both complexes are strictly conserved.

Stereospecific Assignment of Aromatic and Methylene Protons. The presence of NOESY cross-peaks between *para* and *meta* tpp phenyl protons in both ytterbium(III) complexes allows us to safely distinguish the *meta* proton pair from the *ortho* proton pair. Within each pair, NOESY and COSY cross-peaks between each *meta* and its neighbor *ortho* proton allow us to discriminate between the two sides of the phenyl ring. The stereospecific assignment of the phenyl protons of **III** can be obtained by analyzing the 1D NOE spectra obtained upon saturation of the methylene protons. As was mentioned earlier, $-CH_2$ protons of oep give small inter-porphyrin NOEs with aromatic protons of tpp (B→D, C→D, and C→G). Signal D was previously assigned as an *ortho* proton signal and signal G as a *meta* proton signal. These inter-porphyrin NOEs thus immediately identify signals D and G as due to tpp phenyl endo

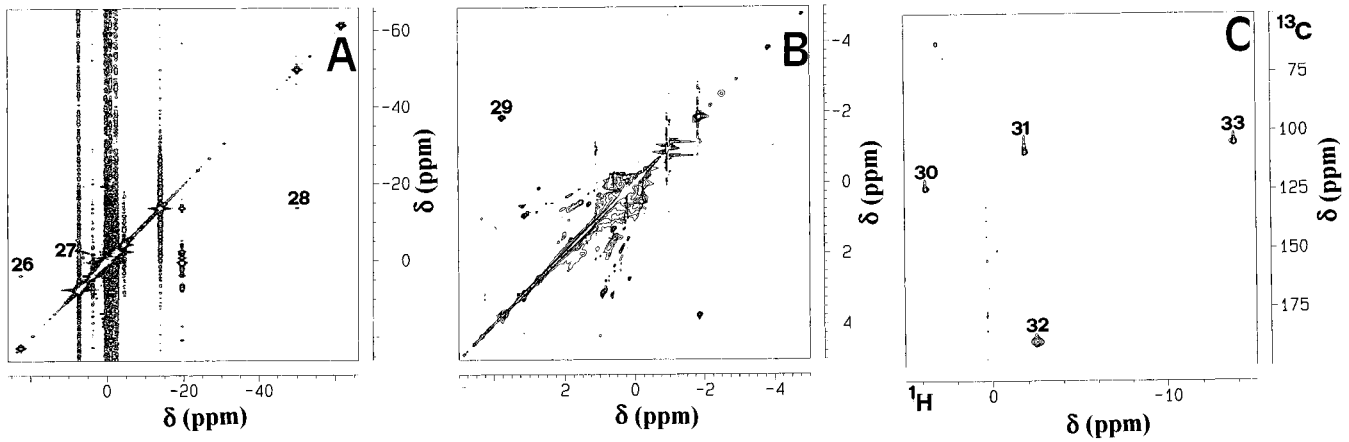

Figure 5. 600 MHz 298 K ^{1}H NMR spectra of [DyH(oep)(tpp)] (**IV**). (A) 2D COSY spectrum. Cross-peak assignments: (26) exo-*ortho*, exo-*meta*; (27) exo-*meta*, *para*; (28) endo-*meta*, endo-*ortho*. (B) 2D TOCSY spectrum with spin lock time of 25 ms. Cross-peak assignment: (29) exo-*meta*, *para*. (C) ^{1}H−^{13}C (natural abundance) HMQC spectrum. Cross-peak assignments: (30) ^{1}H exo-*meta*, ^{13}C exo-*meta*; (31) ^{1}H *para*, ^{13}C *para*; (32) ^{1}H methyl, ^{13}C methyl; (33) ^{1}H endo-*meta*, ^{13}C endo-*meta*.

protons, *i.e.* tpp phenyl protons facing the oep ring. Therefore, signals E and H are due to phenyl exo *ortho* and *meta* protons, respectively. We also note that, although the differences in T_1 values between endo and exo protons are small because they are almost completely averaged by ring flips, they are consistent with the present stereospecific assignment. The stereospecific assignment for the tpp phenyl protons of **I** cannot be obtained, because of the lack of inter-porphyrin NOEs in this case.

The COSY and TOCSY patterns observed for the dysprosium(III) complexes **II** and **IV** also allow us to differentiate between the *ortho* and the *meta* proton pairs, and between the two *ortho*−*meta* neighbor pairs. In this case, no inter-porphyrin NOEs could be detected, and the T_1 values inside each diastereotopic pair are too similar to help in performing the stereospecific assignment. However, advantage can be taken from the known geometric relationship between the phenyl protons and the lanthanide. As the *z* axis of the χ tensor is imposed by symmetry to lie on the C_4 axis of the complex, the value of the θ angles of each ring protons with the *z* axis can be calculated. It appears that the θ value is smaller than the magic angle value of 54°74′ for the exo *ortho* protons (≅50°), larger for the exo *meta* (≅58°), and progressively larger for the *para* (≅73°), endo *meta* (≅86°) and endo *ortho* (≅89°) protons. Therefore, the sign of the hyperfine shift of the exo *ortho* protons should be opposite to that of the other protons. Among the *meta* protons, the endo *meta* protons should have the larger absolute value. This reasoning is valid for both complexes **II** and **IV**. As a result, the stereospecific assignment given in Tables 2 and 4 is achieved.

The stereospecific assignment for methylene protons of **III** can be obtained by analyzing the intensities of the NOEs observed upon irradiation of both $-CH_2$ and *meso* protons of the *oep* ring. By comparison of the intensities of the NOEs obtained upon saturation of A (*meso* proton) we observe that the NOE with signal B is larger than that with signal C. Consistently, by saturating B we observe a small NOE with the *meso* proton A, while no NOE on A could be detected upon saturation of C (Figure 2). Furthermore, signal C gives stronger NOEs with the endo *ortho* and *meta* aromatic protons of the tpp ring (signals D and G, Figure 2), than signal B does. Signal B has a shorter T_1 than signal C. These observations suggest that the methylene protons are made distinguishable by some preferred orientation of the ethyl groups, in such a way that one of them (B) is, on the average, closer to the *meso* proton and to the metal ion, and the other (C) is closer to the phenyl ring of tpp. We term the former endo and the latter exo methylene protons. The absence of NOEs involving the methylene protons of **IV** prevent us from obtaining their stereospecific assignment.

Further information on the preferred orientation of the ethyl groups in the asymmetric complex **III** in solution can be obtained from 1D NOE experiments. In the solid state, the structure of [SmH(oep)(tpp)] shows six methyl groups in the exo position and two in the endo position, but there are no particular symmetry or steric requirements for this situation to be maintained in solution for both complexes. The inter-ring NOE on the oep methyl protons obtained by saturating the tpp pyrrolic proton signals of complex **III** (Figure 2) indicates that the methyl groups must point for a nonnegligible fraction of time toward the tpp ring; i.e., they must spend a fraction of time in the endo position. Indeed, the distance between a tpp pyrrole proton and a methyl group in the exo position if far too large to permit the observation of the NOE between them. By taking as a reference the known intra-ring distance between pyrrolic and exo-*ortho* protons (Figure 2) and the intensity of the NOE between them, we could reproduce the observed inter-ring NOE intensity between pyrrolic and methyl protons by assuming that each methyl group spends, on the average, one-fourth of the time in the endo orientation. This result is in amazingly good agreement with the solid state data on the samarium(III) complex.

No NOE between pyrrolic and methyl protons is detected in complex **IV**. This finding may be due to the larger paramagnetism of the latter complex, which makes the observation of small NOEs intrinsically more difficult. Alternatively, it could be due to a smaller fraction of time spent by the methyl groups in the endo position in complex **IV** with respect to complex **III** and to the samarium(III) complex in the solid state. We consider the latter possibility rather unlikely. A qualitative comparison of the T_1 values for corresponding protons in **III** and **IV** whose distance from the metal is fixed (pyrrole, *meso*, and *para* protons) reveals a ratio of about 4−5, not far for the ratio of 4.1 predicted from the $J(J + 1)$ ratio for the two ions. The ratio of the T_1 values of the methyl groups is 4.3, suggesting that their endo/exo ratio is similar in both complexes. Finally, we note that the T_1 values of methylene and *ortho* exo phenyl protons deviate sizably from the predicted ratio of 4.1; the latter even give a result slightly shorter than the corresponding endo *ortho* protons. The reasons for these deviations are unclear at the moment, although ligand-centered relaxation effects from the porphyrin π system may be responsible for an anomalous behavior of this type.

Table 5. Experimental Hyperfine Shifts and Calculated Pseudocontact Shifts[a] for [DyH(tpp)$_2$] (**II**) and [DyH(oep)(tpp)] (**IV**) Complexes

	[DyH(tpp)$_2$]		[DyH(oep)(tpp)]	
assignment	exptl hyperfine shift, ppm	calcd[b] pseudocontact (contact) shift, ppm	exptl hyperfine shift, ppm	calcd[c] pseudocontact (contact) shift, ppm
exo-*ortho*	15.1	13.2	16.2	13.4
exo-*meta*	0.1	−1.1	−3.4	−1.1
para	-9.7	−9.4	−9.6	−9.5
CH_3[d]			−3.8	−10.3 (6.5)
endo-CH_2[d]			−6.6	−30.4 (23.8)
exo-CH_2[d]			−8.2	−30.7 (22.5)
meso[d]			−21.7	−75.3 (53.6)
endo-*meta*	−18.5	−20.8	−21.9	−21.1
endo-ortho	−59.7	−59.4	−59.3	−60.3
pyrrolic[d]	−61.0	−28.5 (−32.5)	−61.4	−29.0 (−32.4)

[a] The reported calculated shifts are averaged. [b] Calculated using $\Delta\chi_{ax} = 1.05 \times 10^{-32}$ m^3. [c] Calculated using $\Delta\chi_{ax} = 1.07 \times 10^{-32}$ m^3. [d] Shifts not taken into account for tensor calculation.

Tensors Calculation. Comparison of the hyperfine shift data in Tables 1−4 shows striking differences between the Yb^{3+} (**I** and **III**) and Dy^{3+} (**II** and **IV**) complexes. The hyperfine shifts of the former are all smaller, but the difference is particularly marked for the phenyl protons of tpp. This behavior is observed for both symmetric and asymmetric complexes. Among all ligand protons, phenyl protons (together with methyl protons) are probably those experiencing the smallest contact contributions, as they are separated by more σ bonds from the porphyrin rings and should experience little π-delocalization due to their essentially orthogonal orientation with respect to the porphyrin plane. The Yb^{3+} complexes display a relatively small paramagnetism, and the phenyl ring protons display very little hyperfine shifts. Their safe analysis would require the precise knowledge of the diamagnetic contribution to the experimental shifts, which is not available except if reference is made to the shifts of the Lu^{3+} complexes. This approach is instead reasonable for the Dy^{3+} complexes, which experience large phenyl proton shifts. Therefore we have chosen to analyze the hyperfine shifts of complexes **II** and **IV**. The average symmetry of both complexes is tetragonal (D_{4d} and C_{4v}, respectively), so that an axial χ tensor must hold, and the *z* axis must lie along the tetragonal axis. The hyperfine shift data for the five inequivalent ring protons of the phenyl groups are thus more than enough to determine the χ tensor parameters if the average orientation of the phenyl groups is taken to be perpendicular to the porphyrin ring and if it is assumed that the contact shift is negligible. This is the usual procedure to analyze the contribution to the hyperfine shifts in tpp complexes.[34,35] The pseudocontact shifts arise from magnetic susceptibility anisotropy, and depend on the nuclear position with respect to the principal axes of the magnetic susceptibility tensor.[36] The five parameters which define the χ tensor anisotropy with respect to any metal-centered axes system can be found by best fitting, to a set of δ_i^{pc} values, the equation[27]

$$\delta_i^{pc} = \frac{1}{12\pi r_i^5}\left[\Delta\chi_{ax}(3(\boldsymbol{r_i}\cdot\boldsymbol{r_z})^2 - \boldsymbol{r_i}^2) + \frac{3}{2}\Delta\chi_{rh}((\boldsymbol{r_i}\cdot\boldsymbol{r_x})^2 - (\boldsymbol{r_i}\cdot\boldsymbol{r_y})^2)\right] \quad (2)$$

where $\Delta\chi_{ax}$ and $\Delta\chi_{rh}$ are the axial and the rhombic anisotropy of the magnetic susceptibility originated by the paramagnetic ion, $\boldsymbol{r_i}$ are the position vectors of the protons relative to the chosen axis system and $\boldsymbol{r_x}$, $\boldsymbol{r_y}$, and $\boldsymbol{r_z}$ are unit vectors along the principal directions of the χ tensor. The five parameters are $\Delta\chi_{ax}$, $\Delta\chi_{rh}$, and three independent direction cosines out of the nine direction cosines defining $\boldsymbol{r_x}$, $\boldsymbol{r_y}$, and $\boldsymbol{r_z}$ in the chosen axis system. In the present case, the orientation of the *z* axis is fixed by symmetry, $\Delta\chi_{rh}$ is zero, again by symmetry, and *x* and *y* axes are not defined. Therefore, we are left with $\Delta\chi_{ax}$ as the only unknown.

The results of the fitting are shown in Table 5 for both complexes. The values of $\Delta\chi_{ax}$ are very similar for both complexes, as expected from the nuclear hyperfine shifts, and the overall agreement is reasonably good. The discrepancies could well be due to residual contact contributions. The substantial agreement confirms that the assumption of perpendicular phenyl rings is correct: if the phenyl rings are allowed to librate over some −10 to +10°, and the average pseudocontact shifts calculated, the differences between positive and negative shifts would be even smaller, contrary to the experimental finding. So, the phenyl rings do rotate, but between two rigid positions.

The methyl groups in **IV** can be treated similarly. The shifts are consistent with a pyrrole−C_α−C_β dihedral angle of ≈80° (i.e. almost perpendicular to the porphyrin ring) in an exo arrangement, slightly tilted toward the mirror plane bisecting the pyrroles. Hyperfine shifts of methyl groups in triple-decker oep−lanthanide complexes have also been interpreted in the same way in the past.[2] However, the results are also consistent with the endo/exo ratio found from NOE and X-ray data, with a 25% population of endo methyl groups at an angle of about −100° and 75% population of exo methyl groups with an angle of about 100°. The latter values are much more consistent with the expected effect of the steric repulsion between ethyl groups on the same pyrrole. The picture that emerges thanks to NOE data is therefore that methyl groups exchange between endo and exo positions and that the exchange is fast on the chemical shift scale. As the hyperfine shifts for the +100 and −100° positions can be calculated from the magnetic anisotropy tensor to be +9 and −34 ppm, respectively, a lower limit for the exchange rate of the methyl groups between the two positions can be set to 10^5 s^{-1}. Such a value is much higher than that obtained for the phenyl ring flip rate.

With the above structural information at hand, the pseudocontact shifts for the other protons of complexes **II** and **IV** (pyrrole protons of tpp and methylene and *meso* protons of oep) can be calculated (Table 5) and the contact shift values can be obtained by difference. Values of δ^{con} of ≈−30 ppm are obtained for pyrrole protons, ≈+25 ppm for methylene protons, and ≈+55 ppm for *meso* protons. These rather large values suggest that small δ^{con} contributions on the other protons cannot be completely ruled out.

(34) La Mar, G. N.; Walker, F. A. In *The Porphyrins*; Dolphin, D., Ed.; Academic Press: New York, 1979; pp 61−157.
(35) Behere, D. V.; Birdy, R.; Mitra, S. *Inorg. Chem.* **1982**, *21*, 386−390.
(36) McConnell, H. M.; Robertson, R. E. G. *J. Chem. Phys.* **1958**, *29*, 1361.

Concluding Remarks

The assignment of the ^{1}H NMR spectra for two ytterbium(III) and two dysprosium(III) porphyrin complexes has been obtained by taking advantage of 1D NOE experiments and 2D spectroscopies. Since the T_2 values may be as small as 1−5 ms, the experiments had to be tailored for fast relaxation. Furthermore, the fast (on the NMR time scale) rearrangements of the ethyl substituents of the oep ring and the slow flip rate of the phenyl substituents of the tpp ring further complicate the assignment. Nevertheless, the combined use of (*i*) longitudinal relaxation which provides information on the metal-proton distances and (*ii*) NOE and ROE experiments which distinguish between H−H dipolar coupling and H−H exchange, together with the detection of scalar coupling, has provided a wealth of structural and dynamic information. In particular, the phenyl rings have been found to flip at a rate of about 30 s^{-1} between two positions as measured on the [YbH(tpp)$_2$] complex. The ethyl groups have been proposed to be quite mobile but to spend, on average, one-fourth of the time in the endo position and three-fourths in the exo position. Finally, the pseudocontact shifts for the dysprosium derivatives have been calculated on the basis of the resulting structural model and found to be satisfactorily close to the experimental ones. As a whole, this research, which has been challenging for the obtainment of good spectroscopic data and for the interpretation of the spectra, has provided a clear picture of the behavior of the investigated complexes in solution.

Acknowledgment. A.D. thanks the International Centre for Genetic Engineering and Biotechnology for a research postdoctoral fellowship. The support of the EU for the visit of G.S. to the FLORMARPARM LSF (ERBCHGECT 940060) to perform the NMR experiments reported in this paper is acknowledged. Financial support from the Italian CNR (Comitato Scienze Chimiche e Comitato Biotecnologie) is acknowledged. This research has also been supported through Grant N 91EΔ442 from the Greek GGET.

IC960339F